

# Preparation and Characterization of Nanoparticle-Filled, Mixed-Matrix Membranes for the Pervaporation Dehydration of Isopropyl Alcohol

C. Venkata Prasad,<sup>1,2</sup> B. Yeriswamy,<sup>3,4</sup> H. Sudhakar,<sup>1</sup> P. Sudhakara,<sup>2</sup> M. C. S. Subha,<sup>3</sup>  
J. I. Song,<sup>2</sup> K. Chowdoji Rao<sup>1</sup>

<sup>1</sup>Department of Polymer Science and Technology, S. K. University, Anantapur 515003, Andhra Pradesh, India

<sup>2</sup>Department of Mechanical Engineering, Changwon National University, Changwon 641773, South Korea

<sup>3</sup>Department of Chemistry, S. K. University, Anantapur 515003, Andhra Pradesh, India

<sup>4</sup>Biomedical Nano materials Laboratory, Department of Polymer Science and Engineering, Pusan National University, Pusan 609735, South Korea

Received 13 April 2011; accepted 15 September 2011

DOI 10.1002/app.35658

Published online in Wiley Online Library (wileyonlinelibrary.com).

**ABSTRACT:** Novel polymeric mixed-matrix membranes (MMMs) were prepared by the incorporation of different amounts of 13X zeolite into a sodium carboxymethylcellulose (NaCMC)/poly(vinyl alcohol) (PVA) blend matrix. The resulting MMMs were characterized by attenuated total reflectance–Fourier transform infrared spectroscopy to analyze the possible chemical reactions between NaCMC, PVA, zeolites, and glutaraldehyde. Scanning electron microscopy, differential scanning calorimetry, thermogravimetric analysis, and X-ray diffraction were used to analyze the surface morphology, thermal stability, and crystallinity, respectively, of the membranes. Swellings studies were performed at 35°C, and we found that membranes containing 20 wt % zeolite showed higher values (960 kg m<sup>-2</sup> h<sup>-1</sup>) at 17.5 wt % water in an isopropyl alcohol (IPA)/water mixture. Pervaporation (PV) experiments were also performed to evaluate the membrane

performance in different compositions of the IPA/water mixture at 35°C. The mechanical properties were also tested, and we found that the optimum mechanical strength and percentage elongation at break were 42.24 N/mm<sup>2</sup> and 3.38, respectively, for the membrane containing 15 wt % zeolite. The experimental results show that both the flux and selectivity increased with increasing zeolite content. The membrane containing 20 wt % zeolite showed the highest separation selectivity (5118) with a substantial flux of 0.121 kg m<sup>-2</sup> h<sup>-1</sup> at 35°C and with 10 wt % water in the feed; this suggested that the membranes could be used effectively to break the azeotropic point of the water–IPA mixture, so as to remove a small amount of water from IPA. © 2012 Wiley Periodicals, Inc. *J Appl Polym Sci* 000: 000–000, 2012

**Key words:** biodegradable; blends; crosslinking

## INTRODUCTION

The separation of water-based mixtures through hydrophilic polymer membranes has been studied extensively. Huang and Jarvis<sup>1</sup> investigated the pervaporation (PV) and separation characteristics of aqueous alcohol solutions through cellophane and poly(vinyl alcohol) (PVA) membranes. Other types of polymer membranes, such as Nafion, sulfonated polyethylene, and sulfonated polypropylene membranes have been studied by Gierke et al.,<sup>2</sup> Cabasso and Liu,<sup>3</sup> and Xu et al.<sup>4</sup> Mulder et al.<sup>5</sup> presented a

membrane-controlled continuous fermentation process for the production of pure ethanol from sugar. The esterification of carboxylic acid with alcohols and the phenol–acetone condensation reaction accompanied by membrane separation have been reported by Okamoto et al.<sup>6</sup> and Neel et al.<sup>7</sup>

PVA has been widely employed in engineering applications because of its ease of preparation, excellent film forming properties, good chemical resistance, physicochemical properties, and biodegradable nature.<sup>8–10</sup> Even though PVA has good mechanical properties in the dry state, its hydrophilicity limits its application as a PV membrane.<sup>11,12</sup> This problem has been overcome by various methods, namely, crosslinking, grafting, and blending.<sup>13–16</sup> Thus, PVA has been chemically modified with aldehydes, carboxylic acids, and anhydrides to improve its hydrophilicity and thermal and mechanical properties.<sup>17,18</sup> Recently, Adoor et al.<sup>19</sup> reported the use of mixed-matrix membranes (MMMs) of PVA containing sodium montmorillonite clay for the PV separation of aqueous–organic mixtures; Khayet et al.<sup>20</sup> reported

Correspondence to: J. I. Song (jisong@changwon.ac.kr) or K. C. Rao (chowdojirao@gmail.com).

Contract grant sponsors: University Grants Commission, New Delhi, India (University Grants Commission–Research Fellowships in Science for Meritorious Students scheme; to C.V.P.), Brain Korea (BK21) Projects Corps of the second phase, Changwon National University, South Korea (to C.V.P.).

the use of poly(2,6-dimethyl-1,4-phenylene oxide) dense membranes filled with silica and silane nanoparticles.

Several reports have been published in the literature on different types of hydrophilic polymers, including PVA, sodium alginate, and chitosan, as membrane materials in the PV separation of the aqueous–organic mixtures.<sup>21–23</sup> Hydrophilic polymers modified with grafting, blending, interpenetrating polymeric networks, and filler-incorporated membranes have been more promising than plain membranes in the PV dehydration of aqueous–organic mixtures.<sup>24–27</sup> Zeolite particles have been used in the development of MMMs because of their intrinsic properties, including their molecular sieving; their thermal resistivity and chemical stability<sup>28</sup> helps to improve their PV performance. Deficiencies in both polymeric and purely molecular sieving media suggest the need for the development of MMMs. Thus, organic–inorganic hybrid membranes have received much attention in PV dehydration.<sup>29</sup> Such MMMs would combine the excellent size-sieving capacity of zeolites with the desired mechanical and processing characteristics of the polymers.

To develop zeolite-filled membranes,<sup>30</sup> we studied the development of MMMs by incorporating various amounts of 13X zeolite particles (5, 10, 15, and 20 wt %) with respect to the weight ratio of sodium carboxymethylcellulose (NaCMC)/PVA. The membranes thus developed could enhance the PV performance over that of plain NaCMC50 blend membranes. The NaCMC/PVA blend (50 : 50) formed the optimum miscibility,<sup>31,32</sup> hence, we chose this composition for the preparation of the MMMs. The results of this study are discussed in terms of the nature of the polymer–filler interaction and liquid molecule components of the mixed media.

## EXPERIMENTAL

### Materials

NaCMC [viscosity = 1100–1900 cps (1 w/v %)] was supplied by Merck (Mumbai, India). PVA (molecular weight = 70,000) was procured from Hi-Media, Mumbai, India. Glutaraldehyde (GA), hydrochloric acid (HCl), isopropyl alcohol (IPA), and acetone, all of analytical grade, were purchased from Qualigens (Mumbai, India). 13X zeolite was supplied from IICT (Hyderabad, India). Double-distilled water collected in the laboratory was used throughout the work.

### Preparation of 13X zeolite filled NaCMC/PVA MMMs

NaCMC and PVA (50 : 50), each 1 g, were dissolved separately in 100 mL of distilled water under con-

stant stirring for about 24 h at ambient temperature to form homogeneous blend solutions. This solution was then filtered with a fritted glass disc filter to remove air bubbles and undissolved matter. The bubbled free blend solution was spread onto a cleaned prelevelled glass plate, kept in a dust-free atmosphere, and allowed to dry at room temperature. The dried membrane was peeled off from the glass plate and crosslinked with 2.5 mL of GA in acetone/water (85 : 10) with concentrated HCl (2.5 mL) as an activator, and the membrane thus formed was designated as NaCMC50. The crosslinking reaction took place between the –OH groups of NaCMC, PVA, and –CHO groups of GA because of the formation of ether linkages by the elimination of water molecules.

To prepare NaCMC/PVA MMMs, various amounts of 13X zeolite particles (5, 10, 15, and 20 wt % with respect to the NaCMC and PVA contents) were added to a NaCMC/PVA (50 : 50) blend solution. A known amount (5 wt %) of zeolite was placed in a beaker containing 10 mL of distilled water and allowed to sonicate in an ultrasonic bath at a fixed frequency of 38 kHz for about 30 min to break up the aggregated crystals of the zeolite particles and to improve the dispersion of zeolite in the blend solution. The product was poured into the previous blend solution and kept under stirring for a further 24 h at room temperature. The membrane was cast onto a glass plate and crosslinked with GA, as explained earlier; the membrane thus formed was designated as NaCMCX5. Repeating the previous procedure, we also prepared additional membranes by varying the zeolite content (at 10, 15, and 20 wt %), and these membranes were designated as NaCMCX10, NaCMCX15, and NaCMCX20, respectively. The thickness of the membrane was measured at different positions with a micrometer screw gauge with an accuracy of  $\pm 2 \mu\text{m}$ , and the average thickness was considered for the calculations. The thickness of various membranes was found to be  $30 \pm 2 \mu\text{m}$ . These dried membranes were used for further characterization and for PV dehydration of the IPA/water mixture of various compositions.

### Swelling properties of the membranes

The interaction of the membranes with the pure liquid components of the feed mixture was determined by gravimetric sorption experiments at 35°C. Weighed samples of circular pieces of crosslinked films (2 cm in diameter) were soaked in pure distilled water and in their binary mixtures for 48 h after the completion of a specified time. The membranes were removed from the bottles, quickly wiped without much pressure with blot paper to remove the adhered liquid, and then weighed immediately. The degree of swelling (DS) was calculated with the following equation:

$$\%DS = \left( \frac{M_s}{M_d} \right) \times 100 \quad (1)$$

where  $M_s$  is the mass of the swollen polymer (g) and  $M_d$  is the mass of the dry polymer (g).

### Mechanical properties

The equipment used for testing the mechanical properties was universal tensile testing machine (Instron 3369) with an operating head load of 5 kN. The cross-sectional area of a sample of known width and thickness was calculated. The films were then placed between the grips of the testing machine for a constant grip length of 5 cm. The speed of testing was set at a rate of 12.5 mm/min.

### Attenuated total reflectance (ATR)–Fourier transform infrared (FTIR) spectroscopy studies

FTIR spectra (Canada) of different membranes were taken with a Bomem MB-3000 FTIR (Canada) spectrometer equipped with ATR. The membranes were characterized at room temperature in the range 4000–600  $\text{cm}^{-1}$  under an  $\text{N}_2$  atmosphere at a scan rate of 21  $\text{cm}^{-1}$ .

### Thermal analysis [differential scanning calorimetry (DSC) and thermogravimetric analysis (TGA)]

DSC (UK) and TGA (UK) curves of NaCMC50 and their MMMs were recorded with a differential scanning calorimeter (TA Instruments, model SDT Q600). The analysis of the samples was performed at a heating rate of 10°C/min under an  $\text{N}_2$  atmosphere (purging speed = 100 mL/min).

### X-ray diffraction (XRD) studies

XRD curves were recorded with a Rigaku Geigerflex diffractometer (Tokyo, Japan) equipped with Ni-filtered  $\text{Cu K}\alpha$  radiation ( $\lambda = 1.548 \text{ \AA}$ ). The dried membranes of uniform thickness were mounted on a sample holder, and the patterns were recorded in the range 0–50° at a speed of 5°/min at Central University (Hyderabad, India).

### Scanning electron microscopy (SEM)

SEM micrograms (Japan) of the membranes were obtained under high resolution (300×, 5 kV) with a scanning electron microscope (JEOL JSM 840A) at Anna University, Chennai, India

## RESULTS AND DISCUSSION

### ATR–FTIR spectroscopy

Figure 1 shows the FTIR spectra of different membranes. Figure 1(A) shows the IR spectra of NaCMC,

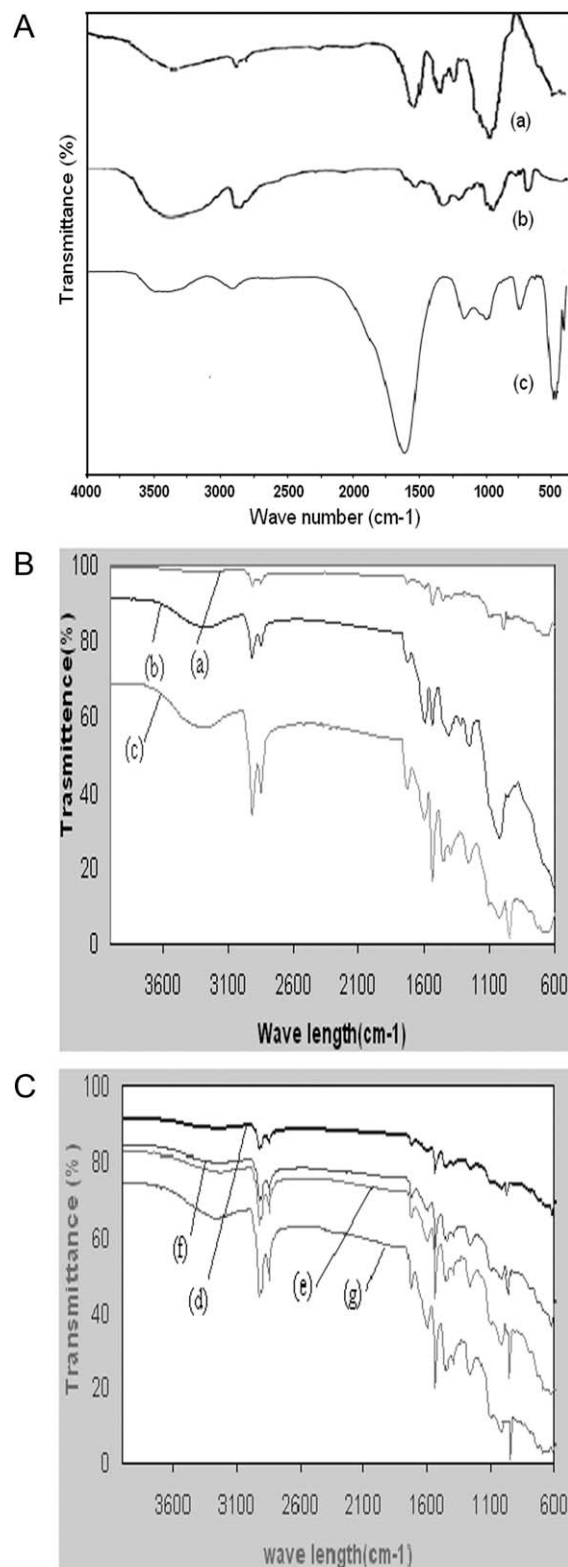


**Figure 1** FTIR spectra (A) (a) plain NaCMC, (b) PVA, and (c) plain 13X zeolite particles; (B) (a) plain NaCMC50, (b) crosslinked NaCMC50, and (c) uncrosslinked NaCMCX10 (c); and (C) (d) crosslinked NaCMCX5, (e) NaCMCX10, (f) NaCMCX15, and (g) NaCMCX20.

PVA, and plain 13X zeolite particles. In the case of plain NaCMC50 [Fig. 1[B(a)]], a broad band observed at  $3336\text{ cm}^{-1}$  was attributed to the O—H stretching vibrations of NaCMC and PVA,<sup>31,32</sup> and this band shifted to  $3342\text{ cm}^{-1}$  in the case of the MMMs [Fig. 1[C(d–g)]] because of the hydrogen-bond interaction between the —OH groups of NaCMC50 and the zeolite particles.<sup>33</sup> Two bands observed at  $2937$  and  $2860\text{ cm}^{-1}$  indicated the presence of C—H aliphatic stretching vibrations. NaCMC50 [Fig. 1[B(a)]] showed a characteristic band at  $3450\text{ cm}^{-1}$  due to O—H stretching vibrations, whereas two bands at  $2928$  and  $2843\text{ cm}^{-1}$  were attributed to C—H aliphatic stretching vibrations. Bands around  $1097$ ,  $802$ , and  $460\text{ cm}^{-1}$  [Fig. 1(a,c)] were attributed to the characteristic silica frame work of 13X zeolite. Peaks around  $3330$  and  $3628\text{ cm}^{-1}$  corresponded to the —OH groups of the 13X zeolite particles (absorbed moisture). In the case of the crosslinked NaCMC50 membrane [Fig. 1[B(b)]], all of the characteristic bands of the uncrosslinked NaCMC50 could be observed in addition a new band at  $1248\text{ cm}^{-1}$ , which was due to the presence of an ether group formed by the reaction of —CH=O of GA with the hydroxyl groups of NaCMC and PVA. These data confirmed the successful crosslinking of the NaCMC50 membrane [Fig. 1[B(c)]]. In the case of the zeolite-filled membranes, an additional peak was observed at  $952\text{ cm}^{-1}$ . This might have been due to the hydrogen-bond formation of NaCMC and PVA with hydroxyl groups of 13X zeolite particles.<sup>33</sup> Furthermore, in the range  $3100$ – $3700\text{ cm}^{-1}$ , the peaks recorded for neat NaCMC [Fig. 1[A(a)]] and PVA [Fig. 1[A(b)]] at  $3385\text{ cm}^{-1}$  were shifted to higher wave numbers, between  $3398$  and  $3436\text{ cm}^{-1}$  [Fig. 1(C)], depending on the zeolite content. Similar results were also reported by Konstantions et al.<sup>33</sup> in the case of PVA/SiO<sub>2</sub> membranes.

## SEM

The typical surface morphologies of plain NaCMC50 and its MMMs are shown in Figure 2. The 13X zeolite incorporated membranes showed uniform distribution up to 15 wt %; beyond this, a concentration increase in aggregation was observed; this increase may have been due to the increase in the concentration of 13X zeolites. In our earlier study, a similar trend was observed in case of 4A zeolite filled NaCMC/PVA (50 : 50) MMMs.<sup>34</sup> Furthermore, the micrograms clearly show that the zeolite particles were embedded in the membrane with no voids.

## DSC

The DSC curves of the pristine NaCMC50 and 13X zeolite filled membranes (NaCMCX5 and NaCMC10X) are shown in Figure 3. The peak at about  $95^\circ\text{C}$  in

curve a was due to the moisture content, and the curve for pristine NaCMC/PVA membrane showed an endothermic peak at  $192.25^\circ\text{C}$ , which corresponded to its melting point. The melting endothermic peak shifted to higher temperatures, that is,  $193.5$  and  $195.3^\circ\text{C}$ , respectively, for the NaCMCX5 and NaCMCX10 membranes. However, an increase in  $T_m$  in the case of the 13X zeolite filled MMMs might have been due to a change in the molecular structure of the membranes (hydrogen-bond formation with —OH groups of PVA); this further led to an increase in  $T_m$  of the 13X zeolite filled membranes.

## TGA

The TGA curves shown in Figure 4 illustrates the thermal stability of NaCMC50 and its MMMs. Three major weight loss stages were observed in all of the membranes; the first weight loss was around  $100^\circ\text{C}$  and was attributed to the loss of absorbed water molecules, which was in agreement with previous studies.<sup>13,34,35</sup> The second weight loss around  $200^\circ\text{C}$  corresponded to the decomposition of NaCMC and PVA chains. The weight loss in the third stage was observed around  $275^\circ\text{C}$  and may have been due to the decomposition of residual carbon chains. The remaining residue (45%) after  $350^\circ\text{C}$  was ascribed the presence of residual carbons and inorganic content. The incorporation of 13X zeolite particles led to strong hydrogen bonding between NaCMC, PVA, and zeolite; this could have dramatically suppressed the decomposition of the NaCMC and PVA chains, and the zeolite-filled membrane exhibited better thermal stability than the pure NaCMC membrane [Fig. 4(a)]. In comparison, the interactions between NaCMC/PVA and 13X zeolite were so weak that the zeolite 13X affected the thermal stability of the NaCMC and PVA chains, and the thermal stability changed with increasing 13X zeolite content [Fig. 4(b)].

## XRD

To study the effect of the zeolite content on the membrane morphology, XRD was employed, and its patterns are presented in Figure 5. The pure NaCMC/PVA membrane exhibited two broad peaks around  $10$  and  $20^\circ$  in the diffraction pattern; this was due to the existence of amorphous and crystalline regions, respectively. With increasing zeolite content, the peak appeared around  $10^\circ$  in pure NaCMC/PVA decreased gradually. This was because of decreased intersegmental spacing due to a shrinkage in cell size. This was further supported by the calculated  $d$ -spacing values, which ranged from  $8.10$  to  $6.27\text{ \AA}$ . In addition, the intensity of the peak appearing around  $20^\circ$  decreased gradually with increasing filler density. This was because of decreased crystalline domains in the membrane matrix because the functional groups (—OH) present in the NaCMC and PVA membrane underwent significant

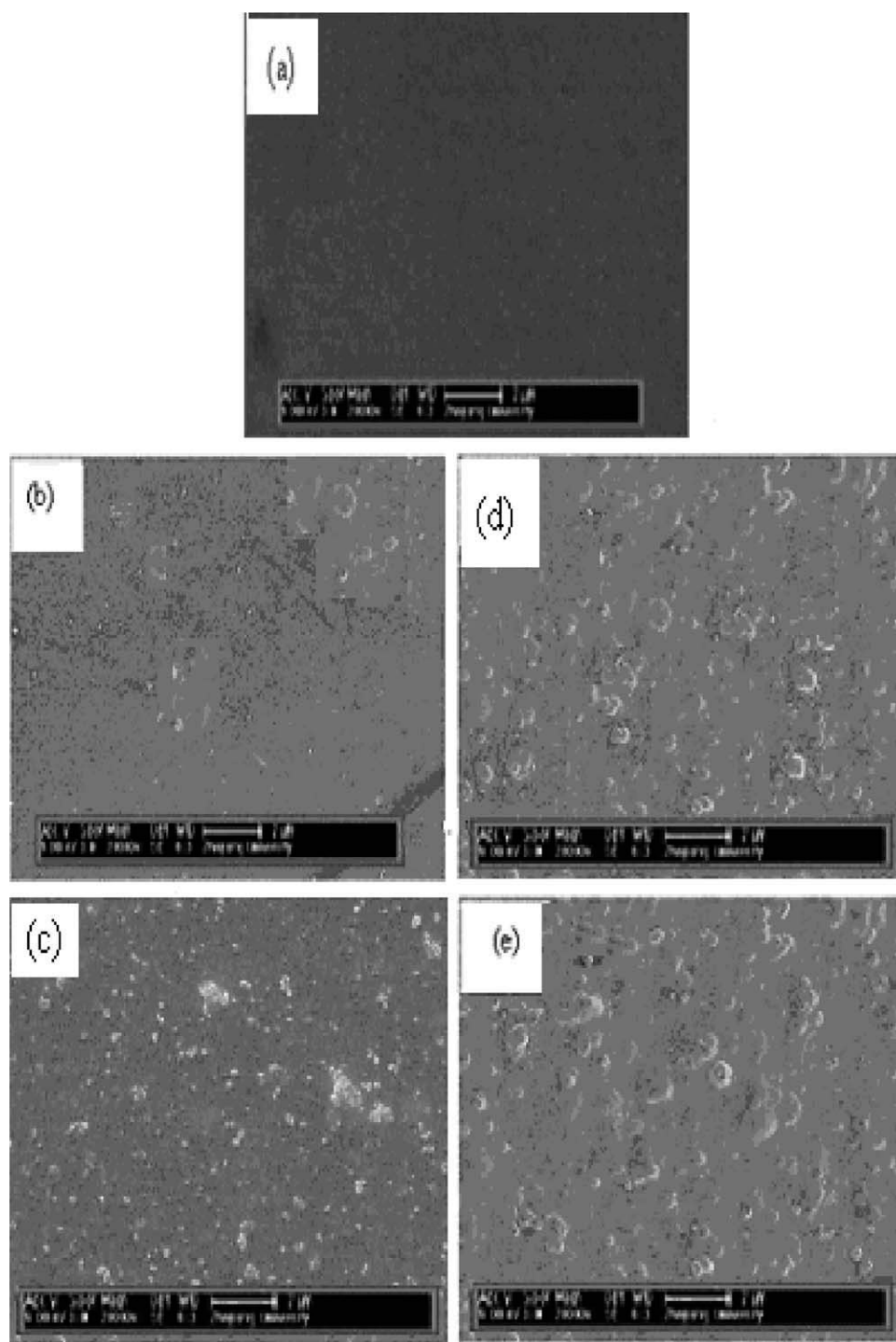


**Figure 2** SEM micrographs of (a) NaCMC50, (b) NaCMCX5, (c) NaCMCX10, (d) NaCMCX15, and (e) NaCMCX20 membranes at 100 $\times$  magnification.

changes after the incorporation of 13X zeolites; these changes resulted in enhanced selective permeation of penetrants through the membranes.

#### Swelling studies

The percentage degree of swelling data obtained from the swelling experiments at 35 $^{\circ}$ C for the plain

NaCMC50 and zeolite filled MMMs was measured as a function of the weight percentage of water in the feed mixtures, and the results are tabulated in Table I and are shown graphically in Figure 6. The efficiency of the membrane depended on its selectivity to the preferred liquid component, namely, water from the water/IPA mixture; this depended on the extent of membrane swelling. Zeolite-filled MMMs

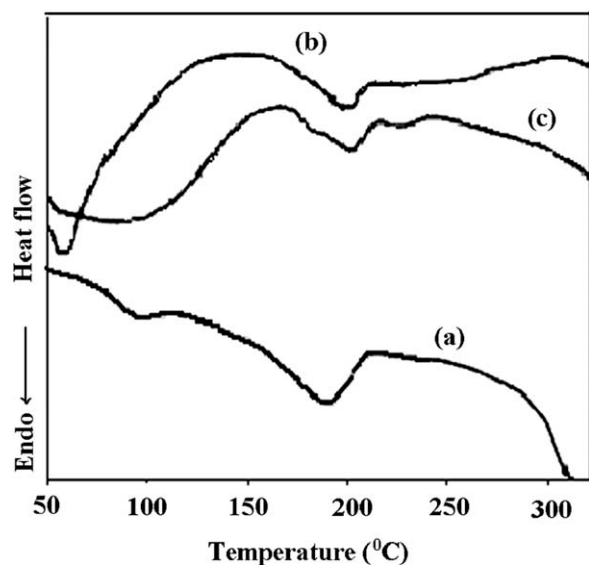


**Figure 3** DSC thermograms of (a) NaCMC50, (b) NaCMCX5, and (c) NaCMCX10 membranes.

showed a higher percentage degree of swelling than the plain NaCMC50 membrane because of their high hydrophilic interactions with water molecules. The fact that the percentage degree of swelling increased with increasing dispersion and zeolite content in the membrane was an indication for the increment in the hydrophilicity of the MMMs. This effect became more prominent when the zeolite dispersion in the membrane increased (Fig. 6). This might have been due to the fact that zeolite had cationic particles, which tended to increase the electrostatic force of attraction between the water molecules and the polymer matrix. This phenomena led to a substantial increase in the adsorption of water molecules, which in turn, was re-

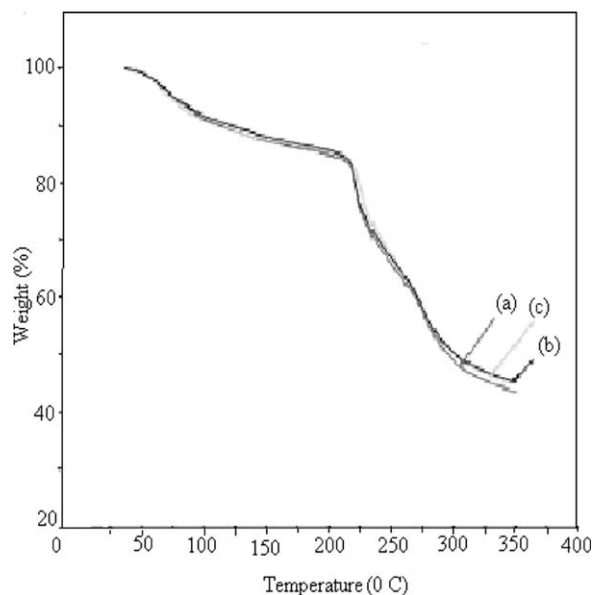


**Figure 4** TGA curves of (a) NaCMC50, (b) NaCMCX5, and (c) NaCMCX10.

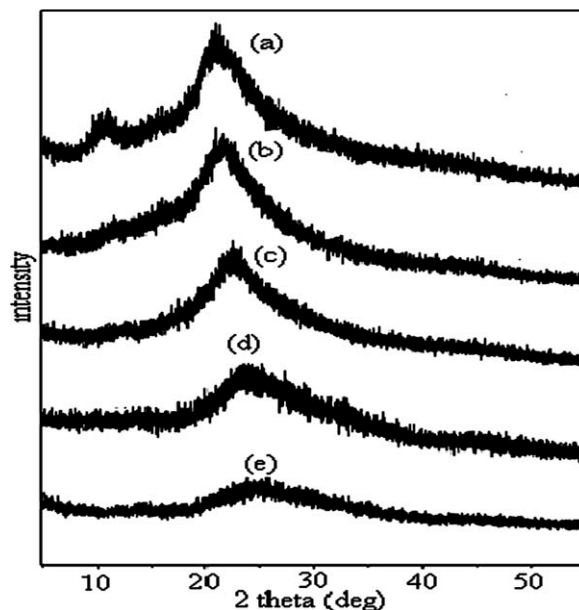


**Figure 5** XRD patterns of (a) NaCMC50, (b) NaCMCX5, (c) NaCMCX10, (d) NaCMCX15, and (e) NaCMCX20 membranes.

sponsible for the increase in swelling with increasing zeolite content in the membranes. A similar observation was also reported by Kariduraganavar et al.<sup>36</sup> in the case of sodium alginate membranes filled with NaY zeolite. In this study, the membrane containing a higher amount of 13X zeolite (20 w/w %) showed a higher percentage of swelling (563–960 kg m<sup>-2</sup> h<sup>-1</sup>) for the feed mixture containing 10–17.5 wt % water.

### Mechanical properties

The mechanical properties of different membranes are shown graphically in Figure 7. The percentage elongation at break of the pristine NaCMC50 was 7.35, whereas the tensile strength was 17.51 N/mm<sup>2</sup>. In the case of the MMMs (NaCMCX5, NaCMCX10, NaCMCX15, and NaCMCX20), the values of the percentage elongation at break and tensile strength were 6.91, 5.43, 3.38, and 2.19 and 18.25, 29.51, 42.24, and 66.98 N/mm<sup>2</sup>, respectively. Extensive intramolecular and intermolecular hydrogen bonding between the —OH groups of zeolite and NaCMC50 and the formation of an interpenetrating polymer network (upon crosslinking) was responsible for such an increase in the tensile strength. It was also observed from the results that as the zeolite content increased in the MMMs, the tensile strength increased continuously from NaCMCX5 to NaCMCX20 (from 18.25 to 66.98 N/mm<sup>2</sup>). The increase in the tensile strength was attributed to the increase in the dispersion of the 13X zeolite particles (with an increase in surface area) with good interfacial adhesion between the zeolite and polymer matrix. The well-dispersed

**TABLE I**  
Swelling Properties of the Various Formulations in Different Water/IPA Feed Mixtures at 35°C

Formulation code	NaCMC/PVA composition (50 : 50)		13X zeolite content (wt %)	Feed water concentration (w/w %)	Degree of swelling (%)
	NaCMC (g)	PVA (g)			
NaCMC50	1	1	0	10	298
				12.5	418
				15.0	513
				17.5	614
NaCMCX5	1	1	5	10	368
				12.5	491
				15.0	580
				17.5	685
NaCMCX10	1	1	10	10	440
				12.5	540
				15.0	697
				17.5	774
NaCMCX15	1	1	15	10	496
				12.5	645
				15.0	765
				17.5	868
NaCMCX20	1	1	20	10	563
				12.5	760
				15.0	856
				17.5	960

zeolite particles had good interactions (intramolecular and inter molecular hydrogen bonding) with the polymer matrix; this resulted in an improvement in the mechanical strength. Membranes containing 20 wt % 13X zeolite showed the optimum tensile strength<sup>37</sup> (66.98 N/mm<sup>2</sup>) and percentage elongation at break (2.19%). Thus, the mechanical strength of the membranes increased with increasing zeolite dispersion in the membrane matrix.<sup>38</sup> The data clearly indicate that the MMMs showed superior mechanical properties.

## PV

The process of PV combines the evaporation of volatile components of a mixture with their permeation

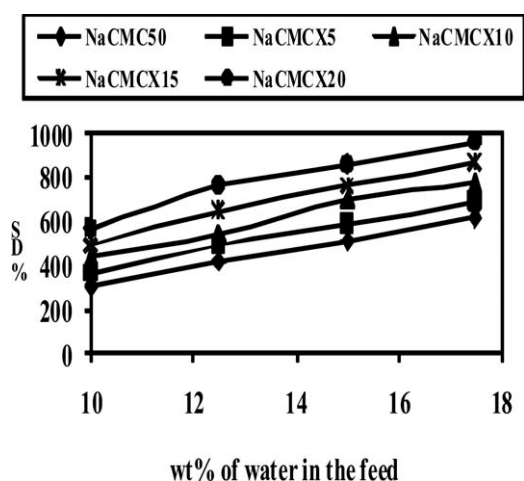


**Figure 6** Effect of the water content on the degree of swelling (SD).

rates through the membrane under reduced pressure. It is well accepted that transport of a volatile substance through a PV membrane involves a sorption step at the membrane upstream face, followed by diffusion through a dense film and desorption into the vacuum side.

## Effect of the zeolite content on the PV performance

The efficacy of the membranes in the PV process is generally assessed on the basis of the permeation of individual components. Therefore, we determined

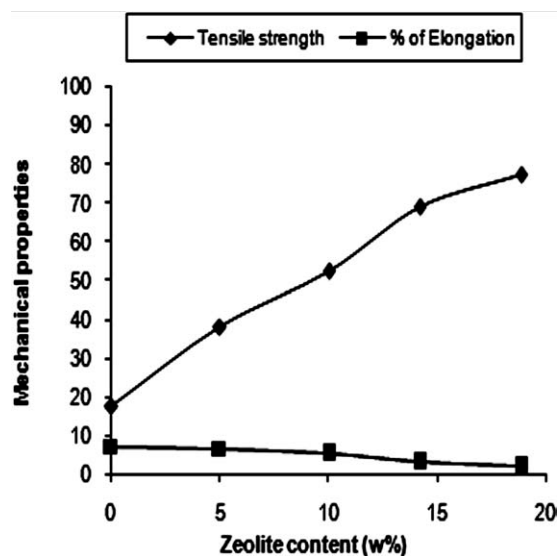


**Figure 7** Effect of the zeolite content on the tensile strength and percentage elongation at break.

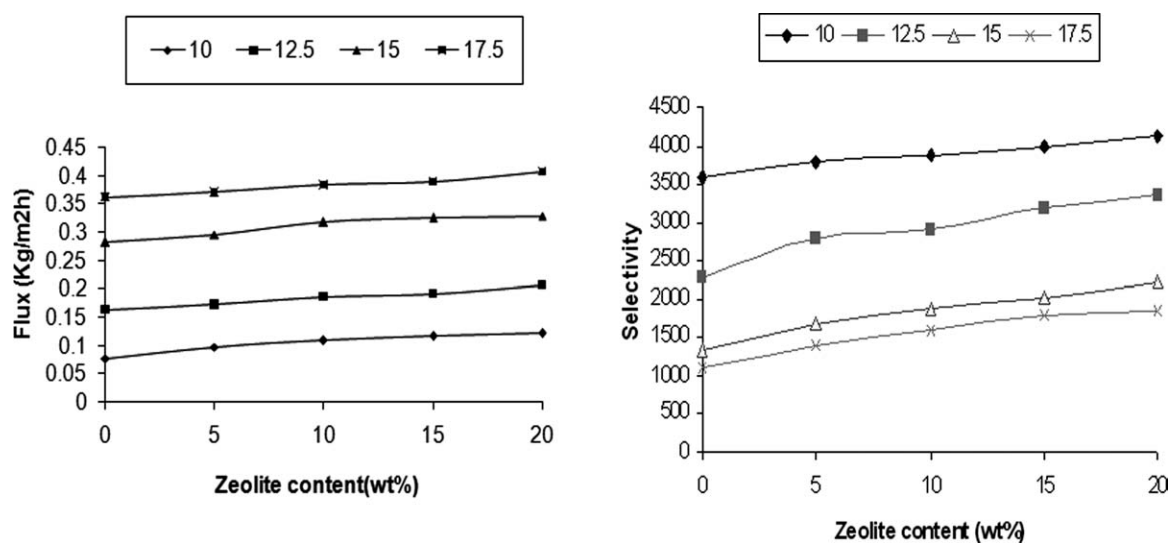


**Figure 8** Effect of the zeolite content on the (a) flux and (b) selectivity at different weight percentages of water in the feed.

the extent of permeation of the individual components by plotting the flux of water as a function of the zeolite content in the membrane for different mass percentages (10, 12.5, 15, and 17.5 mass%) of water in the feed. The results are shown graphically in Figure 8(a). From the plots, it is clearly evident that the flux of water increased with increasing zeolite content for all of the membranes over the entire studied range of water composition. The results indicate that membranes developed in this study were highly water selective. This clearly reveals that the amount of zeolite incorporated into the membrane prominently enhanced the membrane performance by increasing the selective transport. Similar results were also reported by Venkata Prasad et al.<sup>35</sup> and Sudhakar et al.<sup>39</sup> in the case of NaCMC/PVA (50 : 50) blend and sodium alginate membranes incorporated with 4A zeolite particles.

Figure 8(b) shows the effect of the zeolite content on the selectivity of the membranes at different mass percentages (10.0, 12.5, 15.0, and 17.5%) of water in the feed. It was clearly evident that the selectivity increased significantly from membrane NaCMCX5 to membrane NaCMCX20 with increasing 13X zeolite content in the membrane. Generally, with increasing packing density of the membrane with increasing zeolite content in the polymer matrix, the selectivity increased.<sup>40,41</sup>

In this study, the selectivity increased with increasing zeolite content in the membrane. To explain, when we used water-selective zeolite-incorporated membranes, the transport of water molecules through the membrane took place in a straight path through the zeolite pores with subsequent adsorption at the feed side followed by desorption at the permeate side; this, in turn was responsible

for the higher water flux. If enough water was present inside the membrane, the zeolite pores were largely occupied by water molecules; this prohibited the IPA molecules from entering the pores of zeolite. Thus, on its way through the membrane, the IPA molecules had to travel around the zeolite pores. The higher water concentration inside the polymer close to the permeate side of the membrane and the fact that water could travel along the straight path and IPA had to follow a more tortuous path acted together to explain the way in which membrane

**TABLE II**  
PV Results of the Water/IPA Mixtures for Different Membranes at 35°C

Formulation code	Feed water		Selectivity	PSI
	concentration (wt %)	Water flux (kg m <sup>-2</sup> h <sup>-1</sup> )		
NaCMC50	10.0	0.076	4580	348.08
	12.5	0.163	2290	373.27
	15.0	0.282	1340	377.88
	17.5	0.363	1100	399.3
NaCMCX5	10.0	0.098	4788	469.224
	12.5	0.172	2781	478.332
	15.0	0.296	1669	494.024
	17.5	0.371	1395	517.545
NaCMCX10	10.0	0.109	4862	529.958
	12.5	0.186	2904	540.144
	15.0	0.318	1878	597.204
	17.5	0.384	1602	615.168
NaCMCX15	10.0	0.116	4981	577.796
	12.5	0.191	3199	611.009
	15.0	0.325	2014	654.55
	17.5	0.390	1789	697.71
NaCMCX20	10.0	0.121	5118	619.278
	12.5	0.206	3357	691.542
	15.0	0.329	2213	728.077
	17.5	0.408	1852	755.616



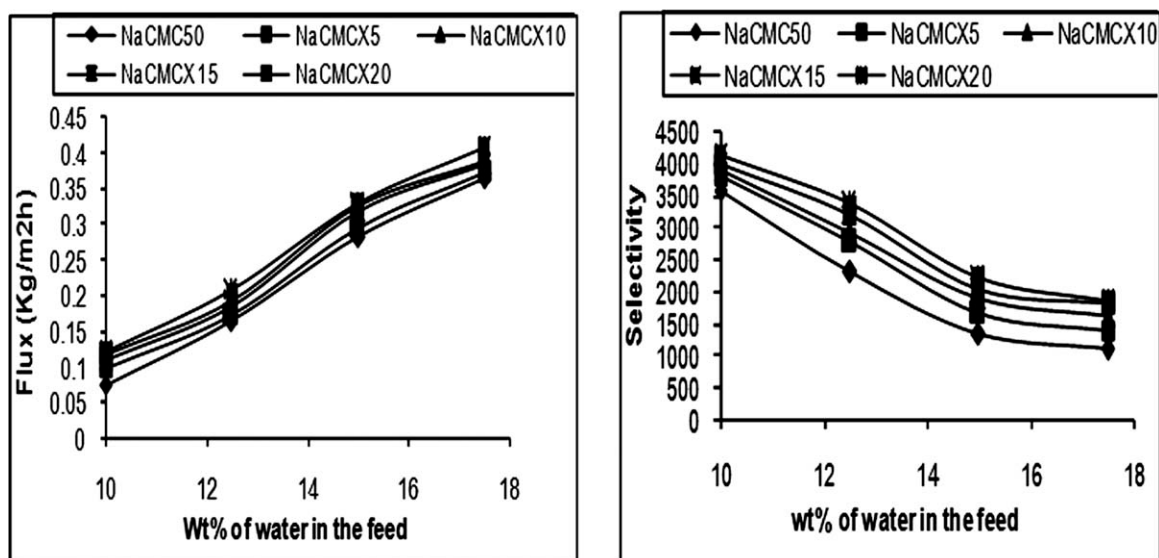


Figure 9 Effect of the weight percentage of water in the feed on the (a) flux and (b) selectivity of different formulations.

performance was enhanced in selectivity when zeolite was added to the polymer matrix.<sup>42</sup> The calculated results of the flux, selectivity, and pervaporation separation index (PSI) of water, measured at 35°C for different compositions with respect to the zeolite loading, in the membranes are presented in Table II. It was observed that there was a systematic increase in the water flux with increasing zeolite loading and water composition in the feed.

PSI is the product of the total permeation and the separation factor; it characterizes the membrane separation ability. This index can be used as a relative guideline for the design of PV membrane separation processes and to select a membrane with an optimum flux and selectivity. The results in Table II indicate that the PSI values increased with increasing zeolite content in the membrane; this signified that the membranes incorporated with a higher amount of zeolite showed better performance for the separation of IPA/water mixtures. This was because the incorporation of zeolite into the membrane matrix did not change only the membrane's hydrophilicity but also its structure; this may have had a significant effect on the diffusion.

#### Effect of the feed composition on the PV performance

PV studies have shown that membrane performance is affected by the water content in the feed mixture. The effects of the feed composition on the PV performance of NaCMC50 and its MMMs are shown in Figure 9(a,b). It was noticed that an increase in the water concentration led to an increase in the permeation flux and, thereby, a decrease in the selectivity. The increase in the flux was due to the preferential interaction of water as the selective component of the feed mixture gave rise to a decrease in selectivity

due to increased swelling.<sup>43</sup> The PV performance of NaCMC50 and its MMMs were investigated in various feed compositions ranging from 10 to 17.5% water with the permeate pressure and membrane thickness kept constant at 0.5 mmHg and 40  $\mu$ m, respectively. Expectedly, a rise in the feed concentration of water produced an increase in the water flux from 0.096 to 0.365 kg m<sup>-2</sup> h<sup>-1</sup> for the NaCMC50 membrane with a drop in selectivity from 4580 to 1100, as shown in Table II. Such a variation in the membrane performance was due to the preferential transport of feed components (an increase in the concentration of water) through the membrane matrix, which produced stronger interactions with the membrane material. This caused the membrane to swell excessively and produced a negative impact on the membrane selectivity because of a plasticizing effect.<sup>44</sup>

## CONCLUSIONS

In this study, we prepared novel hydrophilic 13X zeolite filled MMMs. The unique structure of the membranes were maintained by strong interaction between the NaCMC, PVA, and 13X zeolite particles. The membranes were used to evaluate the PV performance at different compositions of an IPA/water mixture. At 20 wt % zeolite content (NaCMCX20), the MMMs maintained their amorphous structure, and the membrane showed the best and most stable PV separation characteristics at azeotropic compositions of the water/IPA mixture.

## References

- Huang, R. Y. M.; Jarvis, N. R. *J Appl Polym Sci* 1970, 14, 2341.
- Gierke, T. D.; Munn, G. E.; Wilson, F. C. *J Polym Sci Polym Phys Ed* 1981, 19, 1687.

3. Cabasso, I.; Liu, Z. Z. *J Membr Sci* 1985, 24, 101.
4. Xu, Y. B.; Lin, S. K.; Liu, S. A. *Chem J Chin Univ* 1990, 11, 1435.
5. Mulder, M. V.; Hendrickman, J. O.; Hegeman, H.; Smolders, C. A. *J Membr Sci* 1983, 16, 269.
6. Okamoto, K.; Semato, T.; Tanaka, K. H. In *Proc Int Cong. Membrane and Membrane Processes*, Chicago 1990, 1 347
7. Neel, J.; David, M. O.; Gref, R.; Nguyen, Q. T.; Bruschke, H.; Shneider, W. In *Proceedings of the International Congress on Membranes and Membrane Processes*, Chicago, Illinois; 1990; Vol. 1, p 344.
8. Hassan, C. M.; Peppas, N. A. *Adv Polym Sci* 2000, 153, 37.
9. Naidu, B. V. K.; Bhat, S. D.; Sairam, M.; Wali, A. C.; Sawant, D. P.; Halligudi, S. B.; Mallikarjuna, N. N.; Aminabhavi, T. M. *J Appl Polym Sci* 2005, 96, 1968.
10. Toti, U. S.; Aminabhavi, T. M. *J Appl Polym Sci* 2002, 85, 2014.
11. Lee, Y. M.; Nam, S. Y.; Kim, J. H. *Polym Bull* 1992, 29, 423.
12. Sridhar, S.; Smitha, B.; Madhavi Latha, U. S.; Ramakrishna, M. *J Polym Mater* 2004, 21, 181.
13. Martien, F. L. *Encyclopedia of Polymer Science and Engineering*; Wiley: New York, 1986; Vol. 17, p 167.
14. Hodge, R. M.; Edward, G. H.; Simon, G. P. *Polymer* 1996, 37, 1371.
15. Liu, M.; Cheng, R.; Quian. *J Polym Sci Part B: Polym Phys* 1995, 33, 1731.
16. Horkay, F.; Zrinyi, M. *Macromolecules* 1982, 15, 1306.
17. Tomihata, E.; Ikeda, Y. *J Polym Sci Part A: Polym Chem* 1997, 35, 3553.
18. Kurkuri, M. D.; Toti, U. S.; Aminabhavi, T. M. *J Appl Polym Sci* 2002, 86, 3642.
19. Adoor, S. G.; Sairam, M.; Manjeshwar, L. S.; Raju, K. V. S. N.; Aminabhavi, T. M. *J Membr Sci* 2006, 285, 182
20. Khayet, M.; Villaluenga, J. P. G.; Valentin, J. L.; Lopez-Manchado, M. A.; Mengual, J. I.; Seoane, B. *Polymer* 2003, 46, 9881.
21. Aminabhavi, T. M.; Naik, H. G. *J Appl Polym Sci* 2002, 83, 273.
22. Naidu, B. V. K.; Krishna Rao, K. S. V.; Aminabhavi, T. M. *J Membr Sci* 2005, 260, 131.
23. Kanti, P.; Srigowri, K.; Madhavi, J.; Smitha, B.; Sridhar, S. *Sep Purif Technol* 2004, 40, 259.
24. Anjali Devi, D.; Smitha, B.; Sridhar, S.; Aminabhavi, T. M. *Sep Purif Technol* 2006, 51, 104.
25. Bhat, S. D.; Aminabhavi, T. M. *Sep Purif Technol* 2006, 51, 85.
26. Veerapur, R. S.; Gudasi, K. B.; Patil, M. B.; Ramesh Babu, V.; Bhat, S. D.; Sairam, M.; Aminabhavi, T. M. *J Appl Polym Sci* 2006, 101, 3324.
27. Veerapur, R. S.; Gudasi, K. B.; Sairam, M.; Shenoy, R. V.; Netaji, M.; Raju, K. V. S. N.; Sreedhar, B.; Aminabhavi, T. M. *J Mater Sci* 2007, 42, 4406.
28. Kurkuri, M. D.; Toti, U. S.; Aminabhavi, T. M. *J Appl Polym Sci* 2002, 86, 3642.
29. Patil, M. B.; Veerapur, R. S.; Patil, S. A.; Madohusoodana, C. D.; Aminabhavi, T. M. *Sep Purif Technol* 2007, 54, 34.
30. Veerapur, R. S.; Patil, M. B.; Gudasi, K. B.; Aminabhavi, T. M. *Sep Purif Technol* 2008, 58, 377.
31. Sheap, A. M. *Egypt J Solids* 2008, 31, 1750.
32. Venkata Prasad, C.; Sudhakar, H.; Yerri Swamy, B.; Venkata Reddy, G.; Reddy, C. L. N.; Suryanarayana, C.; Prabhakar, M. N.; Subha, M. C. S.; Chowdoji Rao, K. *J Appl Polym Sci* 2011, 120, 2271.
33. Konstantions, C.; Paraskevopoulos, K. M.; Papageorgiou, G. Z.; Bikiaris, D. N. *J Appl Polym Sci* 2008, 110, 1739.
34. Venkata Prasad, C.; Yerri Swamy, B.; Sudhakar, H.; Sobha Rani, T.; Sudhakar, K.; Subha, M. C. S.; Chowdoji Rao, K. *J Appl Polym Sci* 2011, 121, 1521.
35. Mukoma, P.; Jooste, B. R.; Vosloo, H. C. M. *J Power Sources* 2004, 136, 16.
36. Kariduraganavar, M. Y.; Kittur, A. A.; Kulkarni, S. S.; Ramesh, K. *J Membr Sci* 2004, 238, 165.
37. Zhong, Y.; Polose, T.; Hetzer, M.; Kee, D. D. *Polym Eng Sci* 2007, 47, 78.
38. Kumbar, S. G.; Prathap, B.; Lata Manjeshwar, S.; Aminabhavi, T. M. *Polymer* 2007, 48, 5417.
39. Sudhakar, H.; Venkata Prasad, C.; Sunitha, K.; Chowdoji Rao, K.; Subha, M. C. S.; Sridhar, S. *J Appl Polym Sci* 2011, 121, 2717.
40. Kittur, A. A.; Kariduraganavar, M. Y.; Toti, U. S.; Ramesh, K.; Aminabhavi, T. M. *J Appl Polym Sci* 2003, 90, 2441.
41. Kurkuri, M. D.; Toti, U. S.; Aminabhavi, T. M. *J Appl Polym Sci* 2002, 86, 3642.
42. Hennepe, H. J. C.; Bargeman, D.; Mulder, M. H. V.; Smolders, C. A. *J Membr Sci* 1987, 35, 39.
43. Nyugen, Q. T.; Neel, J.; Clement, R.; Leblanc, L. *J Membr Sci* 1983, 15, 43.
44. Huang, R. Y. M.; Yeom, C. K. *J Membr Sci* 1991, 62, 59.